

Regio- and Stereochemical Aspects of the Substitution Reaction between the Molybdenocene and Tungstenocene Dichlorides ($\eta^5\text{-C}_5\text{H}_4\text{-R}$)₂MCl₂ (R = CMe₃, SiMe₃; M = Mo, W) and Metallophosphide Anions [(CO)₅M'PPh₂]₂Li (M' = Mo, W)

Virginie Comte, Olivier Blacque, Marek M. Kubicki, and Claude Moïse*

Laboratoire de Synthèse et d'Electrosynthèse Organométalliques, UMR 5632 (LSEO),
Faculté des Sciences Gabriel, Université de Bourgogne, 21000 Dijon, France

Received June 11, 2001

The reaction of metallophosphide anions [(CO)₅M'PPh₂]₂Li (M' = Mo, W) with the metallocene dichlorides ($\eta^5\text{-Cp}'$)₂MCl₂ (M = Mo, W; Cp' = C₅H₄-CMe₃ (noted **-CM**) or C₅H₄-SiMe₃ (noted **-SiM**)) leads to complexes ($\eta^5\text{-Cp}''$)($\eta^5\text{-Cp}'$)MHCl (Cp'' = C₅H₃-1-R-3-PPh₂M'-(CO)₅), which arise from a nucleophilic substitution on the cyclopentadienyl ligand. The reaction is partially (molybdenocene series) or completely (tungstenocene series) diastereogenic. In solution, a slow transformation of kinetic to thermodynamic products is detected in the molybdenum derivatives, while their tungsten homologues show a total stereostability. On the basis of X-ray structures and of NMR data the relative configurations of the stereoisomers are established.

Introduction

For several years, a part of our work has been turned to the synthesis and the structural characterization of bimetallic systems including different modes of linkage between the two transition metals. We have given examples of μ -phosphido, μ -hydrido, and μ -carbonyl bridged complexes with or without direct interactions between the metallic nuclei.¹ Our general strategy is based on the use of metalloligands containing a metal σ -bonded phosphido group, which allows binding with various organometallic fragments. In the same field, we have recently discovered the ability of metallophosphide anions to undergo a direct Cp substitution on neutral molybdenocene and tungstenocene dichlorides ($\eta^5\text{-C}_5\text{H}_5$)₂MCl₂.² To determine the influence of steric and electronic factors on this unexpected Cp ring nucleophilic substitution, the reaction has been extended to substituted ($\eta^5\text{-C}_5\text{H}_4\text{-tBu}$)₂MCl₂³ and *ansa* [X($\eta^5\text{-C}_5\text{H}_4$)₂]MCl₂ (X = CMe₂, SiMe₂)⁴ metallocene dichlorides (M = Mo, W). Striking differences between these two types of complexes have been observed, notably concerning the site of the reaction: the CMe₂ *ansa*-bridged complex shows substitution at the metallic center, whereas the other metallocene dichlorides show Cp substitution. Although these observations could be attributed to Cp ring tilting variations,⁵ it seemed to us reasonable to

extend these works to other precursors and to get information about the stereochemical course of metallophosphide anion condensation.

Results and Discussion

(A) Tertiobutyl-Substituted Complexes. As we have reported in a previous paper, the reaction of metallophosphide anions [(CO)₅M'PPh₂]₂Li (M' = Cr, Mo, W) with dichlorides ($\eta^5\text{-C}_5\text{H}_4\text{-tBu}$)₂MCl₂ (M = Mo **1-CMo**, = W **1-CW**) undergoes a 1,3 Cp ring substitution.³ A noticeable difference of behavior is observed between molybdenum and tungsten derivatives: the former gives rise to a mixture of two diastereoisomers **2-CMo** and **2'-CMo** (ratio 3:1) (Scheme 1), whereas a complete diastereoselectivity is obtained with the tungsten dichloride ($\eta^5\text{-C}_5\text{H}_4\text{-tBu}$)₂WCl₂ (**1-CW**) (Scheme 2). When the mixture of diastereoisomers **2-CMo** and **2'-CMo** is kept in a THF solution for several hours at room temperature, a complete transformation into the isomer **2'-CMo** takes place, suggesting for **2-CMo** and **2'-CMo** a kinetic and a thermodynamic nature, respectively. In contrast, when allowed to stand in the same conditions, the isolated tungsten **2-CW** derivative shows no evolution. Although more experiments are needed to afford information (*vide infra*) to explain the behavior observed for the tungstenocene derivative, we searched to establish unambiguously the relative configuration of the isolated diastereoisomer. Therefore a solid-state structure of **2b-CW** was determined via a single-crystal X-ray diffraction study (Figure 1). The configuration at tungsten is designated as *R_W* according to the following priority: Cl > Cp' > Cp > H; an *S_P* configuration is assigned to the

* Corresponding author. E-mail: claude.moise@u-bourgogne.fr.

(1) Boni, G.; Kubicki, M. M.; Moïse, C. *Metal Clusters in Chemistry*; Braunstein and Oro, Raithby Eds.; 1999; Vol. 1, p 110–123.

(2) (a) Rigny, S.; Leblanc, J.-C.; Moïse, C. *New J. Chem.* **1995**, *19*, 145. (b) Rigny, S.; Leblanc, J.-C.; Moïse, C.; Nuber, B. *New J. Chem.* **1997**, *21*, 469. (c) Rigny, S.; Bakhmutov, V. I.; Nuber, B.; Leblanc, J.-C.; Moïse, C. *Inorg. Chem.* **1996**, *35*, 3202.

(3) Comte, V.; Rigny, S.; Moïse, C. *Bull. Soc. Chim. Fr.* **1997**, *134*, 609.

(4) Comte, V.; Blacque, O.; Kubicki, M. M.; Moïse, C. *Organometallics* **1997**, *16*, 5763.

(5) Stern, D.; Sabat, M.; Marks, T. J. *J. Am. Chem. Soc.* **1990**, *112*, 9558.

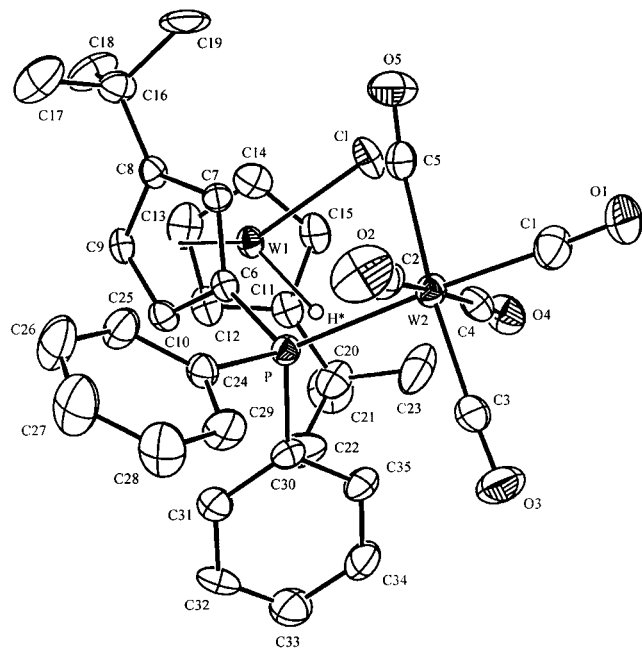
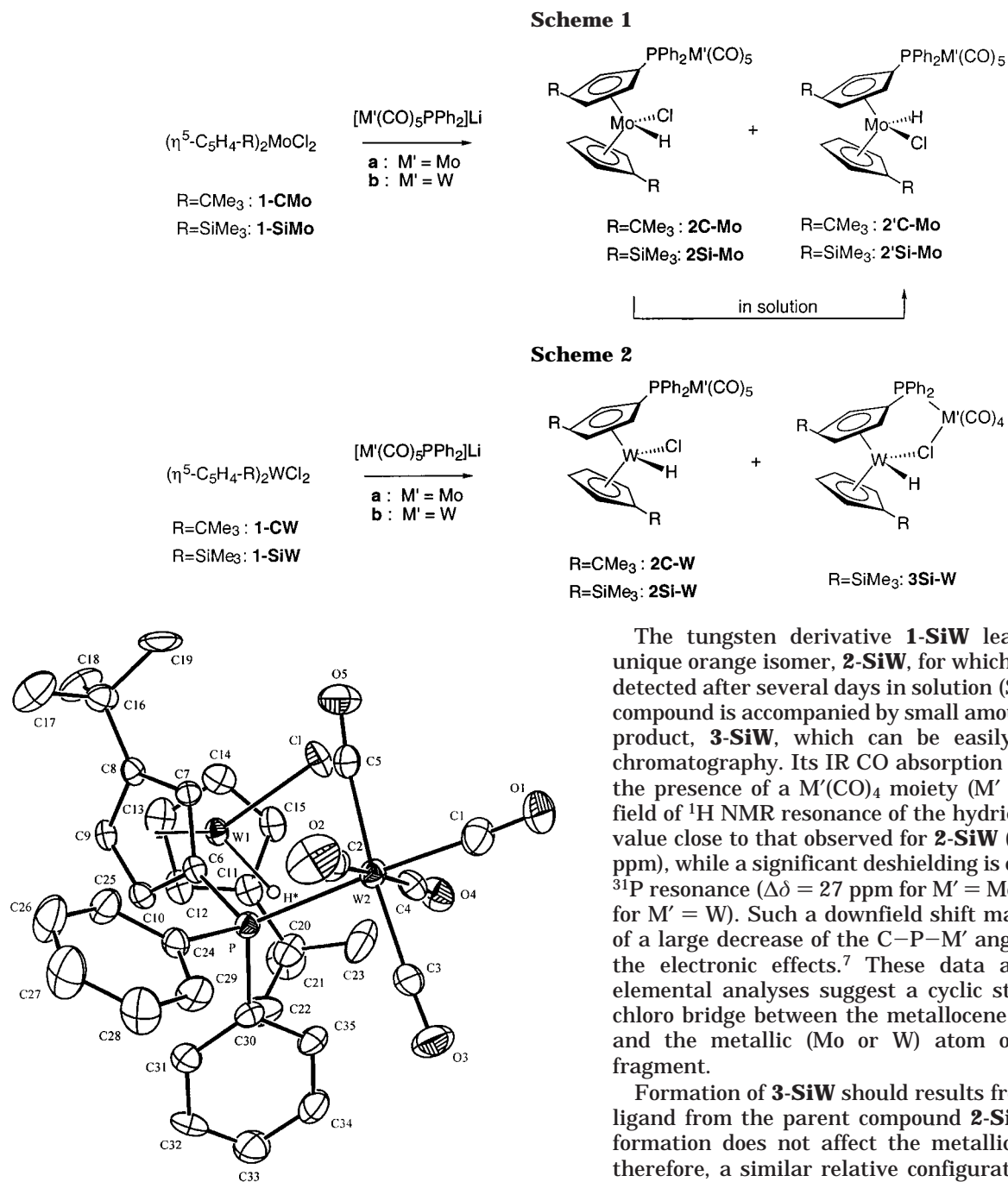


Figure 1. Molecular structure of **2b-CW**.

planar chirality according to the rule edited by Schlägl for chiral ferrocene derivatives.⁶

(B) Trimethylsilyl-Substituted Complexes. When exposed to metallophosphide anions ($\text{M}' = \text{Mo}, \text{W}$), the trimethylsilylated molybdenocene dichloride $(\eta^5\text{-C}_5\text{H}_4\text{-SiMe}_3)_2\text{MoCl}_2$, **1-SiMo**, gives rise, as its tert-butyl homolog, to a mixture of two diastereoisomers, **2-SiMo** and **2'-SiMo** (ratio 3:1) (Scheme 1). The 1,3-disubstitution is clearly established by their NMR data. A slow evolution of **2-SiMo** \rightarrow **2'-SiMo** is displayed in a THF solution but remains incomplete (ratio 1:3), thus precluding the isolation of a pure sample of **2'-SiMo**.

The tungsten derivative **1-SiW** leads again to a unique orange isomer, **2-SiW**, for which no evolution is detected after several days in solution (Scheme 2). This compound is accompanied by small amounts of a second product, **3-SiW**, which can be easily separated by chromatography. Its IR CO absorption pattern reveals the presence of a $\text{M}'(\text{CO})_4$ moiety ($\text{M}' = \text{Mo}, \text{W}$). The field of ^1H NMR resonance of the hydride remains at a value close to that observed for **2-SiW** ($-10.5 \rightarrow -11.5$ ppm), while a significant deshielding is observed for the ^{31}P resonance ($\Delta\delta = 27$ ppm for $\text{M}' = \text{Mo}$ and $= 40$ ppm for $\text{M}' = \text{W}$). Such a downfield shift may be indicative of a large decrease of the C–P–M' angle as well as of the electronic effects.⁷ These data associated with elemental analyses suggest a cyclic structure with a chloro bridge between the metallocene tungsten atom and the metallic (Mo or W) atom of the carbonyl fragment.

Formation of **3-SiW** should result from a loss of CO ligand from the parent compound **2-SiW**. This transformation does not affect the metallic chirality, and therefore, a similar relative configuration is expected for both compounds **2-SiW** and **3-SiW**. This assumption has been proved correct by performing the X-ray structure determinations of suitable crystals of **2b-SiW** and **3b-SiW**. According to the previously stated rules, the ORTEP views show a relative configuration $R_{\text{W}}S_{\text{P}}$ for the both structures **2b-SiW** (Figure 2) and **3b-SiW** (Figure 3). **2b-SiW** crystallizes with two independent molecules in the asymmetric unit of the cell, only differing in relative orientations of the Me groups of the SiMe_3 substituents.

A comparison of the molecular structures of **2b-CW** (Figure 1) and **2b-SiW** (Figure 2) (Table 1) shows a significant difference in their molecular conformations. For the compound **2b-CW**, the *tert*-butyl substituents of the two Cp ligands lie on the opposite sides with

(6) Schlägl, K. *Top. Stereochem.* **1967**, *1*, 39. The observer looks above the disubstituted Cp ring and determines if the two substituents descend in priority in the shortest clockwise (R_{P}) or counterclockwise (S_{P}) way.

(7) (a) Barré, C.; Kubicki, M. M.; Moise, C. *Phosphorus, Sulfur Silicon* **1993**, *77*, 49. (b) Kubicki, M. M.; Le Gall, J. Y.; Kergoat, R.; Gomes de Lima, L. C. *Can. J. Chem.* **1987**, *65*, 1292.

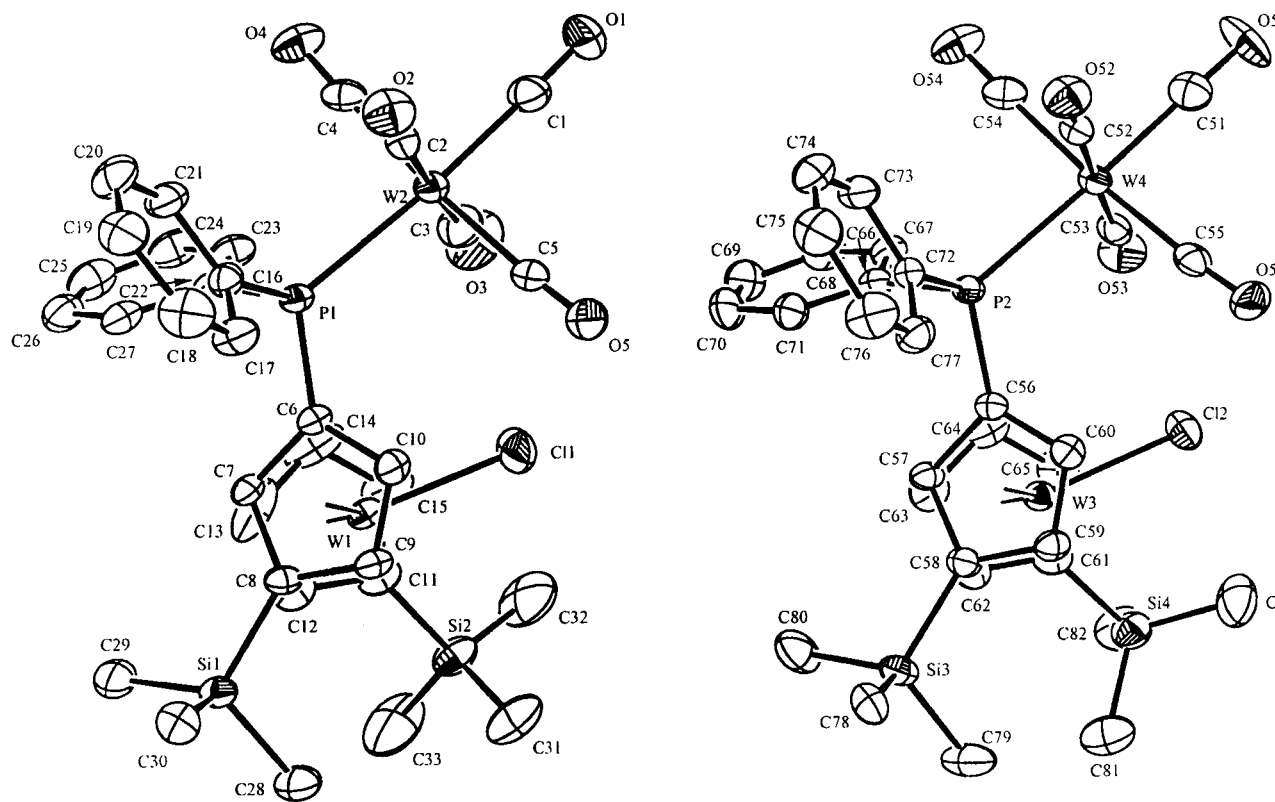


Figure 2. Molecular structure of **2b-SiW**.

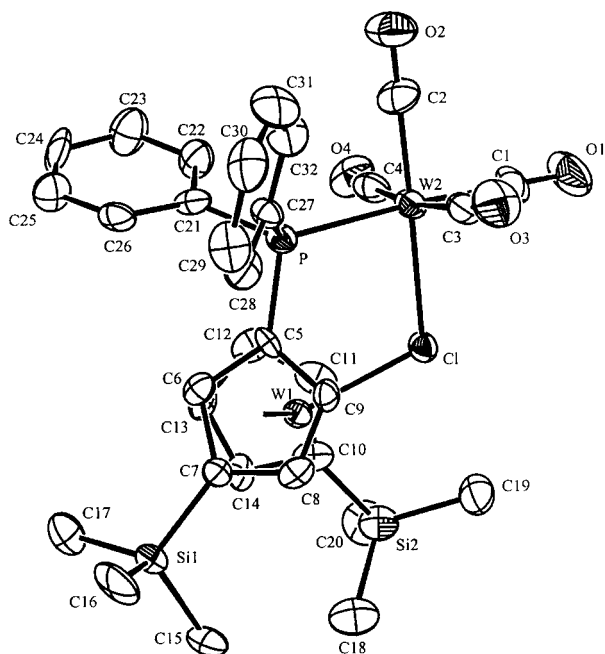


Figure 3. Molecular structure of **3b-SiW**.

respect to the plane defined by the Cp ring centroids and the tungsten atom, whereas in **2b-SiW** the silyl groups are much closer and located on the same side of this plane. This observation shows that less steric hindrance exists with silylated substituents in accord with the smaller cone angle value for the monosubstituted cyclopentadienyl ($C_5H_4-SiMe_3$) of 118° versus 127° for the $C_5H_4-CMe_3$ ligand.⁸ Similar relative positions of $SiMe_3$ substituents are also found in the μ -chloro-bridged derivative **3b-SiW**. Therefore, the lack of formation of chloro-bridged compounds in the *tert*-

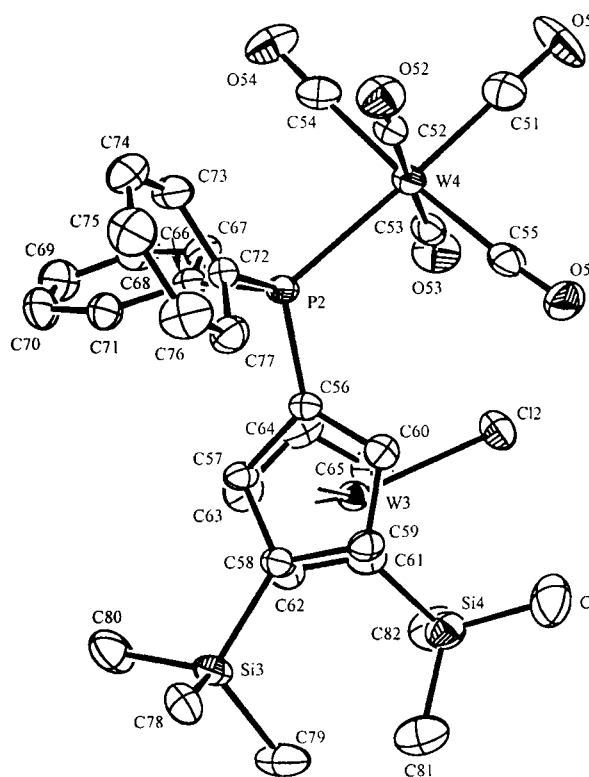


Table 1. Selected Bond Length (\AA) and Angles (deg) for **2b-CW** and **2b-SiW**

	2b-CW	2b-SiW
W1[3]–W2[4]	5.141	5.202 [5.135] ^a
W1[3]–CP1[3]	1.961	1.944 [1.951]
W1[3]–CP2[4]	1.968	1.963 [1.965]
W1–H*	1.63(7)	
W1[3]–Cl1[2]	2.468(2)	2.467(2) [2.455(2)]
W2[4]–P1[2]	2.547(2)	2.538(2) [2.533(2)]
P1[2]–C6[56]	1.825(9)	1.808(6) [1.825(6)]
CP1[3]–W1[3]–CP2[4]	141.62	143.8 [144.2]
W2[4]–P1[2]–C6[56]	119.5(3)	121.6(2) [120.4(2)]
Cl1–W1–H*	79(2)	

^a Values in brackets are for the second (W3/W4) molecule.

butyl series might be due to steric effects, which hinder the rings from reaching a conformation with both substituents (*t*Bu) on the same side of the CP/W/CP plane.

(C) Irradiation of 2/2'-Mo and 2-W Complexes. The behavior of complexes **2-SiW**, which undergo a loss of CO ligand leading to chloro-bridged compounds, prompted us to investigate the evolution under irradiation of molydenocene (**2/2'-CMo** and **2/2'-SiMo**) and tungstenocene (**2-CW** and **2-SiW**) derivatives. Whatever the nature, *tert*-butyl or trimethylsilyl, of the Cp substituents, the irradiation process gives rise to a mixture of two components, **3** and **3'**, in a 1:2 ratio (Scheme 3). An NMR analysis of mixtures formed from **2-SiW** clearly shows that the lesser component corresponds to the samples **3-SiW** produced during the condensation

(8) (a) Blacque, O. Ph.D. Thesis, Université de Bourgogne, Dijon, 1999. (b) Coville, N. J.; Loonat, M. S.; White, D.; Carlton, L. *Organometallics* **1992**, *11*, 1082. (c) Cambridge Structural Database System, 3D Graphics Version for Unix Platforms. Database V5.17, April 1999 Release.

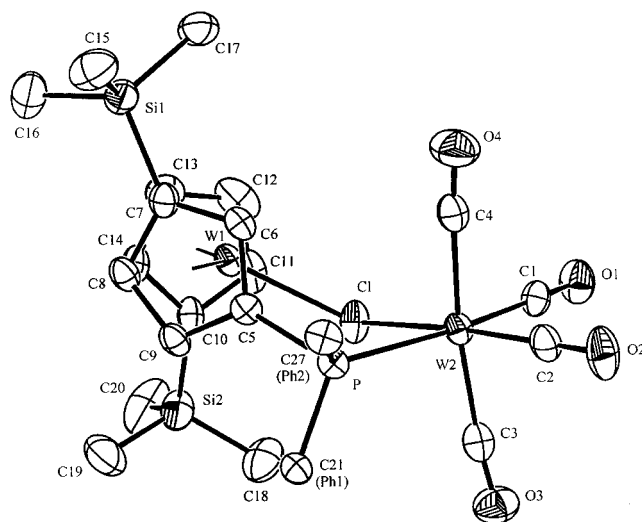
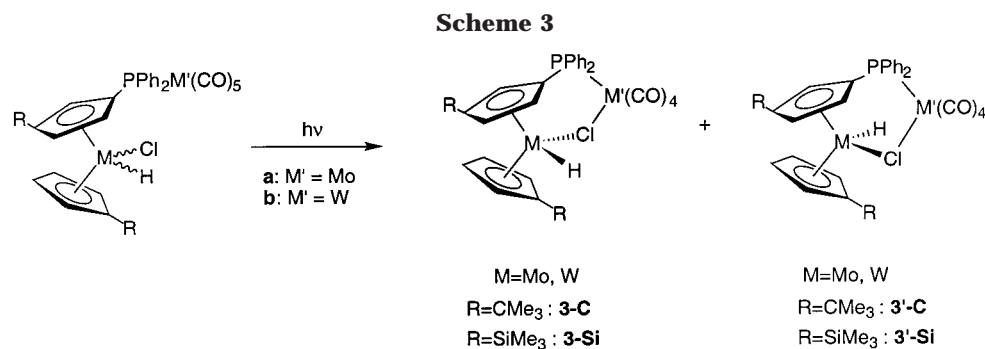


Figure 4. Molecular structure of **3'b-SiW**.

of metallophosphide anions. Furthermore, interesting are the spectroscopic features that appear in the 1H NMR spectra for each couple of diastereoisomeric chloro-bridged compounds **3** and **3'**. The predominant isomer **3'** (-**CM** or -**SiM**; $M = Mo, W$) exhibits a singlet for the hydride resonance, whereas in **3** (-**CM** or -**SiM**; $M = Mo, W$) the signal appears as a doublet ($^4J_{PH} = 4$ to 8 Hz) and is more deshielded ($\Delta\delta$ 0.5 to 1 ppm). These repetitive data are representative of two well-defined isomers: $R_{(Mo,W)Sp}$ and its opposite $S_{(Mo,W)Sp}$. These configurations can be assigned respectively to all the minor **3** and all the major **3'** components of the irradiated mixture.

The X-ray determination of **3'b-SiW**, obtained as the major product from the irradiation mixture of **2b-SiW**, shows an S_{WSp} configuration (Figure 4) and affords definitive proof for the configurational assignments proposed above. Comparison of the diastereoisomeric structures **3b-SiW** and **3'b-SiW** reveals significant differences in the lengths of $W2-P$ and $W2-Cl$ bonds (Table 2). Shorter distances are found in **3'b-SiW** together with an opposite conformation of the two trimethylsilyl substituents. A higher stability for the S_{WSp} isomer **3'-SiW** is probably associated with these structural features.

The chloro bridges are easily cleaved when allowed to react with donor ligands.⁹ With CO, the reaction proceeds in a stereospecific way and quickly regenerates the $M'(CO)_5$ fragment (Scheme 4). When the reaction

Table 2. Selected Bond Length (\AA) and Angles (deg) for **3b-SiW** and **3'b-SiW**

	3b-SiW	3'b-SiW
W1–W2	4.252(1)	4.4305(8)
W1–CP1	1.939	1.967
W2–CP2	1.971	1.952
W1–Cl	2.506(4)	2.494(2)
W2–Cl	2.616(4)	2.570(2)
W2–P	2.537(4)	2.514(2)
P1–C5	1.80(1)	1.825(7)
CP1–W1–CP2	143.5	143.5
W2–P–C6	110.5(5)	111.6(2)
Cl–W2–P	87.2(1)	79.90(6)
W1–Cl1–W2	112.2(1)	122.03(7)

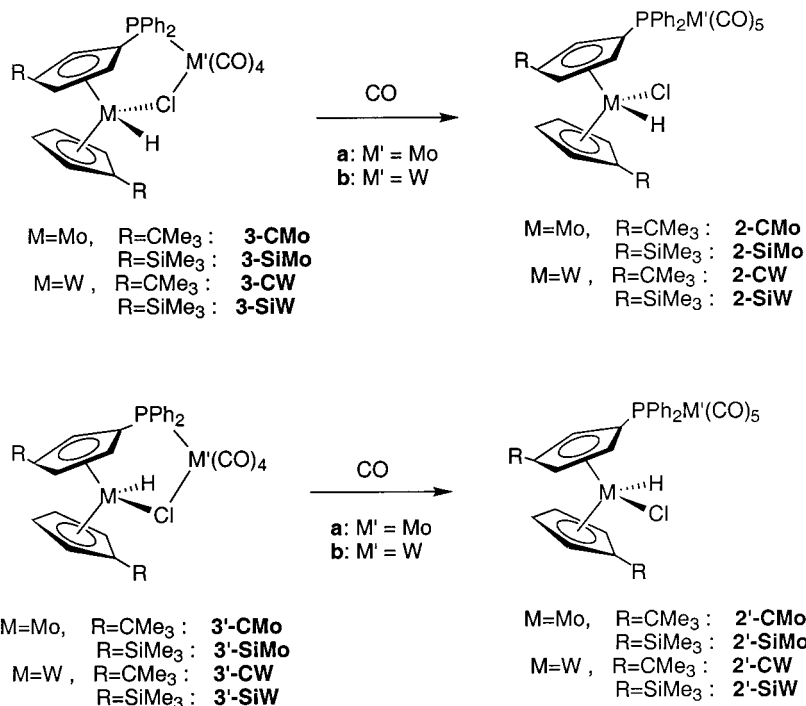
is performed from the μ -chloro tungstenocene derivatives **3'-W**, it becomes possible to isolate complexes **2'-W**, which proves to be the diastereoisomers of products derived from the direct condensation of metallophosphide anions (**2-W**). In solution (THF or toluene), all these isomers display a total configurational stability. This finding allows us to conclude that the condensation of $[(CO)_5M'PPh_2]Li$ anions on substituted tungstenocene dichlorides **1-CW** and **1-SiW** occurs with a complete diastereoselectivity.

NMR data of all the complexes prepared either by direct condensation (**2-CW** and **2-SiW**) or by cleavage of chloro bridges (**2'-CW** and **2'-SiW**) show special features concerning the chemical shifts (1H and ^{31}P) of *tert*-butyl or trimethylsilyl groups, of hydrides, and of bridging phosphorus resonances (Table 3). One group (**2-CW** and **2-SiW**) brings together complexes that exhibit more shielded Cp substituents (CMe_3 or $SiMe_3$) and both more deshielded hydride and phosphorus nuclei with respect to the second group (**2'-CW** and **2'-SiW**), where an opposite trend is observed. The two X-ray structures shown in Figures 1 and 2 correspond to two complexes of the former group (**2-CMo**, **2-SiMo**, **2-CW**, and **2-SiW**) for which therefore the relative configuration R_{MSp} can be ascertained; the opposite configuration, S_{MSp} , is assigned to all members of the other kind of complexes (**2'-CMo**, **2'-SiMo**, **2'-CW**, and **2'-SiW**).

On the basis of these configurational assignments, it can be deduced that the stereochemical course of the metallophosphide condensation is the same whatever the nature of the metallocene involved in the reaction: the kinetic product exhibits an R_{MSp} (+ $S_M R_P$) configuration (**2-Mo** and **2-W** complexes). However, a difference appears between the molybdenocene and tungstenocene series in the evolution to the thermodynamic product: no epimerization is observed with the tungstenocene derivatives.

(9) Comte, V.; Kubicki, M. M.; Moise, C. *Eur. J. Inorg. Chem.* **1999**, 2029.

Scheme 4


Table 3. Comparison of NMR Data for the Complexes 2/2'-Mo and 2/2'-W

complex	¹ H (ppm, CDCl ₃)		³¹ P (ppm, CDCl ₃)
	tBu or SiMe ₃	M-H	
2b-CMo	1.09, 1.22	-7.65	9.74
2'b-CMo	1.25, 1.44	-7.79	8.39
2b-CW	0.90, 1.23	-9.86	10.80
2'b-CW	1.29, 1.47	-10.18	10.04
2b-SiMo	0.09, 0.19	-7.72	8.85
2'b-SiMo	0.13, 0.34	-7.76	7.88
2b-SiW	0.09, 0.22	-10.48	10.24
2'b-SiW	0.12, 0.36	-10.54	9.54

Cleavage of chloro bridges can be also achieved by phosphines (Scheme 5). An example is provided by the reaction of complexes **3b-SiW** and **3'b-SiW** with PMe₃ and PPh₃. Both phosphines give rise to products in which the incoming phosphorus ligand lies in a cis configuration, as indicated by the IR absorption pattern (four CO bands) together with the weak ²J_{PP} coupling constant (≈20 Hz).¹⁰ Considering the above results, the relative configurations of these products are obviously identical to those of their respective precursors.

Conclusion

This work shows that the *tert*-butyl- and the trimethylsilyl-disubstituted molybdenocene and tungstenocene dichlorides give rise to a Cp condensation when opposed to metallophosphide anions. Such an orientation is also found with the unsubstituted metallocene dichlorides, whereas CMe₂-ansa derivatives give substitution on the metal. It seems clear therefore that this nucleophilic substitution is mainly governed by steric and not by electronic factors. Obviously, this reaction affords the opportunity to prepare a wide range

of bimetallic complexes containing a molybdenocene or tungstenocene moiety and to test cooperative interactions between the two metals. Works in this area are currently in progress.

Experimental Section

General Comments. All reactions were carried out under an atmosphere of purified argon. The solvents and eluents were dried by the appropriate procedure and distilled under argon from sodium and benzophenone immediately before use. Standard Schlenk techniques and conventional glass vessels were employed. Column chromatography was performed under argon with silica gel (70–230 mesh). Elemental analyses were carried out with a EA 1108 CHNS-O FISONs instruments. Electron ionization mass spectra were run on a Kratos Concept 32S. ¹H (200 MHz), ³¹P (81 MHz), and ¹³C (50 MHz) spectra were collected on a Bruker AC 200 spectrometer. Chemical shifts are relative to internal TMS (¹H, ¹³C) or external H₃-PO₄ (³¹P). IR spectra were recorded a Nicolet 205 IR-FT. The lithium reagent, [(CO)₅M'PPh₂]₂Li (M' = Mo, W), was prepared according to the literature method¹¹ using low-chloride methyllithium (Janssen). (η⁵-C₅H₄-SiMe₃) was made by the method of Abel and Dunster,¹² and the cyclopentadienyl-lithium reagent was prepared by the action of MeLi on (η⁵-C₅H₄-SiMe₃) in ether as solvent. The complexes **2/2'-CMo** and **2-CW** were already described.³ PMe₃ and PPh₃ (Strem) were used as received.

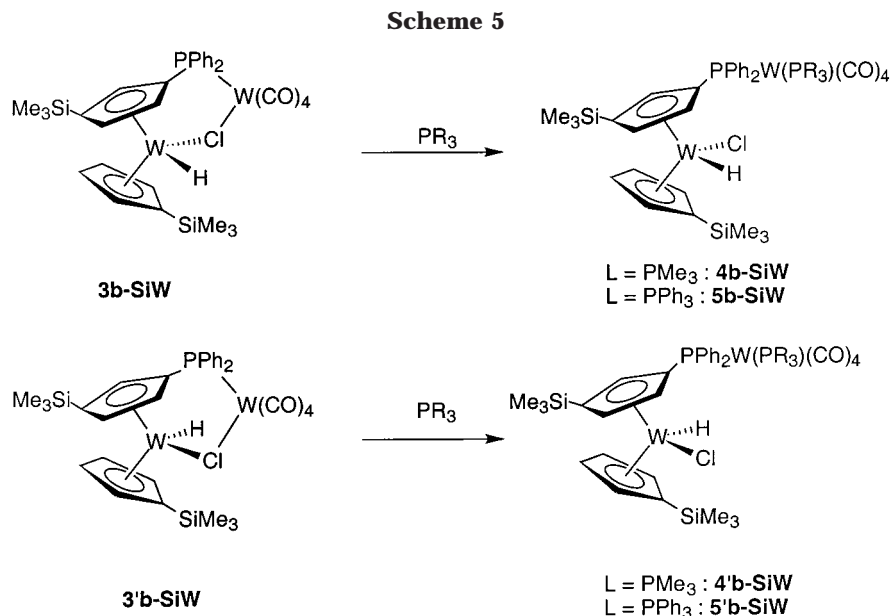
Irradiation Procedure. A solution of the product (1 mmol) in THF (100 mL) was irradiated with a HANAU TQ 150-Hg lamp with a DURAN 50 immersion tube. A nitrogen purge was used to expel the released CO, and the reaction was monitored by IR in the carbonyl stretching region. The irradiation was stopped when no more M'(CO)₅ bands appeared. The necessary time of irradiation was about 2 h.

X-ray Crystallography. All measurements have been carried out at 296(2) K on an Enraf-Nonius CAD4 diffractometer, using Mo Kα graphite-monochromated radiation (λ =

(10) (a) Pregosin, P. S.; Kunz, R. W. *³¹P and ¹³C NMR of Transition Metal Phosphine Complexes*; Springer-Verlag: Berlin, 1979; p 116. (b) Mercier, F.; Hugel-Le Goff, C.; Mathey, F. *Organometallics* **1988**, *7*, 955.

(11) Breen, M. J.; Shulman, P.; Geoffroy, G. L.; Rheingold, A. L.; Fultz, W. C. *Organometallics* **1984**, *3*, 782.

(12) Abel, E. W.; Dunster, M. O. *J. Organomet. Chem.* **1971**, *33*, 161.

**Table 4. Crystal Data for 2b-CW, 2b-SiW, 3b-SiW, and 3'b-SiW**

	2b-CW	2b-SiW	3b-SiW	3'b-SiW
empirical formula	C ₃₅ H ₃₆ ClO ₅ PW ₂	C ₃₃ H ₃₆ ClO ₅ PSi ₂ W ₂ ·1/2C ₃ H ₆ O	C ₃₂ H ₃₆ ClO ₄ PSi ₂ W ₂	C ₃₂ H ₃₆ ClO ₄ PSi ₂ W ₂
fw, g	970.76	1031.96	974.91	974.91
color	red	red	orange	red
cryst size, mm	0.20 × 0.15 × 0.10	0.53 × 0.37 × 0.37	0.20 × 0.20 × 0.17	0.25 × 0.20 × 0.10
cryst syst	monoclinic	triclinic	monoclinic	triclinic
space group	<i>P2</i> ₁ / <i>c</i>	<i>P1</i>	<i>P2</i> ₁ / <i>c</i>	<i>P1</i>
<i>a</i> , Å	11.155(1)	15.685(2)	11.649(1)	10.926(1)
<i>b</i> , Å	13.988(2)	16.668(2)	16.408(2)	11.460(1)
<i>c</i> , Å	22.829(2)	17.305(2)	20.851(3)	16.582(2)
α, deg		85.83(1)		76.39(11)
β, deg	92.403(8)	71.238(9)	92.40(1)	75.81(1)
γ, deg		64.854(9)		63.463(9)
<i>V</i> , Å ³	3559.0(7)	3867.1(8)	3981.8(8)	1782.0(3)
<i>Z</i>	4	4	4	2
calcd density, g cm ⁻³	1.812	1.774	1.624	1.817
abs coeff, mm ⁻¹	6.617	6.155	5.970	6.670
abs corr	ψ-scans	ψ-scans	none	ψ-scans
transmn min/max	77.92/99.82	70.26/99.90		69.70/99.99
<i>F</i> (000)	1864	1992	1872	936
θ range, deg	2.30–26.29	2.25–26.33	2.32–26.34	2.11–26.27
scan type	ω	ω	ω	ω
no. of reflns measd	7608	16 265	8446	7489
no. of indep reflns	7227	15 666	8046	7228
	<i>R</i> _{int} = 0.0478	<i>R</i> _{int} = 0.0248	<i>R</i> _{int} = 0.0915	<i>R</i> _{int} = 0.0317
obsd reflns (<i>I</i> > 2σ(<i>I</i>))	4017	11 528	3807	4778
goodness of fit on <i>F</i> ²	0.986	1.055	1.014	1.007
<i>R</i> indices (<i>I</i> > 2σ(<i>I</i>))				
<i>R</i> 1	0.0430	0.0335	0.0615	0.0333
w <i>R</i> 2	0.0742	0.0768	0.1637	0.0677
largest diff peak, hole e Å ⁻³	0.868, -1.213	0.908, -0.897	1.708, -1.18	1.096, -1.306

0.71073 Å). The unit cells were determined from 25 reflections selected by the CAD4 routines.¹³ Relevant crystal and data collection parameters are summarized in Table 1. The structures were solved by using standard Patterson methods, least-squares refinement (on *F*²), and Fourier techniques. The calculations were performed with the software package SHELX-97.¹⁴ Absorption corrections were made by the psi-scan method for complexes **2b-CW**, **2b-SiW**, and **3'b-SiW**. All non-hydrogen atoms were refined with anisotropic thermal parameters. The hydrogen atoms were placed in their calculated positions and refined with a riding model, except for the hydride ligand in **2b-CW**, which was located in a Fourier difference map and

freely refined with an isotropic temperature factor. The hydride ligands in the other complexes **2b-SiW**, **3b-SiW**, and **3'b-SiW** were not found and then not included in the models. Crystallographic data are gathered in Table 4.

(η^5 -C₅H₄-SiMe₃)₂MCl₂, **M** = Mo **1-SiMo**, = W **1-SiW**. (η^5 -C₅H₄-SiMe₃)₂MCl₂ have been prepared from MCl₄L (**M** = Mo, L = (OEt)₂; **M** = W, L = DME) and Li[η^5 -C₅H₄-SiMe₃] according to the procedure used by Green et al.¹⁵ and isolated pure after recrystallization from chloroform. **1-SiMo**: 65% yield, dark brown powder. ¹H NMR (CDCl₃): δ 5.88 (m, 4H, C₅H₄), 5.21 (m, 4H, C₅H₄), 0.18 (s, 18H, Me). MS (EI) *m/z*: 442 [M⁺]. Anal. Calcd for C₁₆H₂₆Cl₂MoSi₂: C, 43.54; H, 5.94. Found: C, 44.0; H, 6.21. **1-SiW**: 80% yield, gray powder. ¹H NMR (CDCl₃): δ 5.95 (m, 4H, C₅H₄), 4.91 (m, 4H, C₅H₄), 0.21

(13) Fair, C. K. *MoLEN, An Interactive Intelligent System for Crystal Structure Analyses*; Enraf-Nonius: Delft, The Netherlands, 19XX.

(14) Sheldrick, G. *SHELX97, Program for the Solution of Crystal Structures*; University of Göttingen: Germany, 1997.

(15) Labella, L.; Chernega, A.; Green, M. L. H. *J. Chem. Soc., Dalton Trans.* **1995**, 395.

C, 47.77; H, 4.24. Found: C, 47.90; H, 4.32. **3b-CW**: IR (ν_{CO} , THF): 2012 (m), 1901 (S), 1883 (S), 1844 (S) cm^{-1} . ^1H NMR (CDCl_3): δ 7.92–7.66 (m, 4H, C_6H_5), 7.48–7.35 (m, 6H, C_6H_5), 5.58 (m, 1H), 5.26 (m, 1H), 4.76 (m, 2H), 4.24 (m, 1H), 4.06 (m, 1H), 3.77 (m, 1H), C_5H_4 or C_5H_3 , 1.23 (s, 9H, tBu), 1.10 (s, 9H, tBu), -11.0 (d, $^1J_{\text{PH}} = 6$ Hz, $^1J_{\text{WH}}$ masked, 1H, W-H). $^{31}\text{P}\{^1\text{H}\}$ NMR (CDCl_3): δ 56.05 (s, $^1J_{\text{WP}}$ masked). **3'b-CW**: 15% yield, 140 mg, red crystals. IR (ν_{CO} , THF): 2012 (m), 1901 (S), 1883 (S), 1844 (S) cm^{-1} . ^1H NMR (CDCl_3): δ 7.92–7.66 (m, 4H, C_6H_5), 7.48–7.35 (m, 6H, C_6H_5), 5.65 (m, 1H), 4.88 (m, 1H), 4.44 (m, 1H), 4.14 (m, 2H), 4.01 (m, 1H), 3.29 (m, 1H), C_5H_4 or C_5H_3 , 1.45 (s, 9H, tBu), 1.31 (s, 9H, tBu), -11.29 (s, $^1J_{\text{WH}} = 57$ Hz, 1H, W-H). $^{31}\text{P}\{^1\text{H}\}$ NMR (CDCl_3): δ 57.66 (s, $^1J_{\text{WP}} = 257$ Hz). $^{13}\text{C}\{^1\text{H}\}$ NMR (CDCl_3): δ 210.8 (d, $J_{\text{CP}} = 3.7$ Hz, 1C, CO), 209.6 (d, $J_{\text{CP}} = 24$ Hz, 1C, CO), 209.1 (d, $J_{\text{CP}} = 3.7$ Hz, 1C, CO), 202.3 (d, $J_{\text{CP}} = 5.5$ Hz, 1C, CO), 140.7 (d, $J_{\text{CP}} = 35$ Hz, 1C, $i\text{-C}_6\text{H}_5$), 140.6 (d, $J_{\text{CP}} = 6.5$ Hz, 1C, $i\text{-C}_6\text{H}_5$), 135.3 (d, $J_{\text{CP}} = 15$ Hz, 2C, $o\text{-C}_6\text{H}_5$), 132.5 (d, $J_{\text{CP}} = 12$ Hz, 2C, $o\text{-C}_6\text{H}_5$), 131.6 (d, $J_{\text{CP}} = 1.8$ Hz, 1C, $p\text{-C}_6\text{H}_5$), 130.1 (d, $J_{\text{CP}} = 1.8$ Hz, 1C, $p\text{-C}_6\text{H}_5$), 129.3 (d, $J_{\text{CP}} = 1.9$ Hz, 2C, $m\text{-C}_6\text{H}_5$), 129.1 (d, $J_{\text{CP}} = 1.9$ Hz, 2C, $m\text{-C}_6\text{H}_5$), 106.9 (s, 1C, $i\text{-C}$), 105.0 (d, $J_{\text{CP}} = 14.7$ Hz, 1C, $i\text{-C}$), 90.5 (s, 1C), 89.8 (s, 1C), 88.5 (d, $J_{\text{CP}} = 1.8$ Hz, 1C), 79.4 (s, 1C), 78.7 (s, 1C), 69.5 (s, 1C), 67.3 (s, 1C), (third $i\text{-C}$ masked), C_5H_3 or C_5H_4 , 32.6 (s, 1C, $\text{C}(\text{CH}_3)_3$), 32.5 (s, 3C, $\text{C}(\text{CH}_3)_3$), 32.3 (s, 1C, CH_3), 32.2 (s, 3C, CH_3). MS (EI): (m/z): 942 [M^+]. Anal. Calcd for $\text{C}_{34}\text{H}_{36}\text{O}_4\text{ClP}_2\text{W}_2$: C, 43.32; H, 3.85. Found: C, 43.60; H, 4.19.

Cleavage of Chloro Bridges. General Procedure for L = CO. The complex **3** or **3'** was stirred in 20 mL of THF at 50 °C under carbon monoxide atmosphere for 2 h. The solvent was then removed under reduced pressure, and each diastereoisomer led to **2** or **2'** as an orange powder. **2'a-SiW**: IR (ν_{CO} , THF): 2072 (m), 1943 (S) cm^{-1} . ^1H NMR (CDCl_3): δ 7.83–7.63 (m, 4H, C_6H_5), 7.55–7.34 (m, 6H, C_6H_5), 5.05 (m, 2H), 4.90 (m, 1H), 4.41 (m, 1H), 3.71 (m, 2H), 3.47 (m, 1H), C_5H_4 or C_5H_3 , 0.36 (s, 9H, Me), 0.12 (s, 9H, Me), -10.60 (s, $^1J_{\text{WH}}$ masked, 1H, W-H). $^{31}\text{P}\{^1\text{H}\}$ NMR (CDCl_3): δ 27.31 (s). MS (EI): (m/z) 916 [M^+]. Anal. Calcd for $\text{C}_{33}\text{H}_{36}\text{O}_5\text{ClP}_2\text{W}_2\text{Si}_2$: C, 43.32; H, 3.97. Found: C, 43.60; H, 3.85. **2'b-SiW**: IR (ν_{CO} , THF): 2071 (m), 1935 (S) cm^{-1} . ^1H NMR (CDCl_3): δ 7.76–7.65 (m, 4H, C_6H_5), 7.55–6.38 (m, 6H, C_6H_5), 5.12 (m, 1H), 5.05 (m, 1H), 4.88 (m, 1H), 4.44 (m, 1H), 3.71 (m, 2H), 3.48 (m, 1H), C_5H_4 or C_5H_3 , 0.36 (s, 9H, Me), 0.12 (s, 9H, Me), -10.54 (s, $^1J_{\text{WH}} = 52$ Hz, 1H, W-H). $^{31}\text{P}\{^1\text{H}\}$ NMR (CDCl_3): δ 9.54 (s, $^1J_{\text{WP}}$ masked). Anal. Calcd for $\text{C}_{33}\text{H}_{36}\text{O}_5\text{ClP}_2\text{W}_2\text{Si}_2$: C, 39.52; H, 3.62. Found: C, 40.0; H, 3.55. **2'b-CW**: IR (ν_{CO} , THF): 2071 (m), 1940 (S) cm^{-1} . ^1H NMR (CDCl_3): δ 7.83–7.35 (m, 10H, C_6H_5), 5.01 (m, 1H), 4.87 (m, 1H), 4.65 (m, 1H), 4.21 (m, 1H), 3.59 (m, 1H), 3.33 (m, 1H), 3.07 (m, 1H), C_5H_4 or C_5H_3 , 1.48 (s, 9H, Me), 1.31 (s, 9H, Me), -10.18 (s, $^1J_{\text{WH}} = 57$ Hz, 1H, W-H). $^{31}\text{P}\{^1\text{H}\}$ NMR (CDCl_3): δ 10.04 (s, $^1J_{\text{WP}}$

masked). Anal. Calcd for $\text{C}_{35}\text{H}_{36}\text{O}_5\text{ClP}_2\text{W}_2$: C, 43.30; H, 3.74. Found: C, 43.15; H, 3.30.

General Procedure for L = PR₃. To a THF solution (20 mL) of **3b-** or **3'b-SiW** (0.5 mmol) was added 1 equiv of the Lewis base L, and the mixture was stirred 2 h at room temperature. The solvent was removed, and the residue was washed with 3 × 20 mL of pentane and dried under vacuum to give an orange powder. All recrystallizations attempted destroyed the complexes after a few days in solution. **L = PMe₃ (4b-SiW)**: IR (ν_{CO} , THF): 2012 (m), 1908 (S), 1890 (S), 1876 (S) cm^{-1} . ^1H NMR (CDCl_3): δ 7.79–7.57 (m, 4H, C_6H_5), 7.47–7.30 (m, 6H, C_6H_5), 5.18 (m, 2H), 4.73 (m, 1H), 4.63 (m, 1H), 4.45 (m, 1H), 4.05 (m, 1H), 3.73 (m, 1H), C_5H_4 or C_5H_3 , 1.18 (d, $^2J_{\text{PH}} = 7.4$ Hz, 9H, PMe), 0.20 (s, 9H, Me), 0.10 (s, 9H, Me), -10.61 (s, $^1J_{\text{WH}} = 60$ Hz, 1H, W-H). $^{31}\text{P}\{^1\text{H}\}$ NMR (CDCl_3): δ 13.80 (d, $^2J_{\text{PP}} = 20$ Hz, $^1J_{\text{WP}} = 247$ Hz, PPh₂), -41.20 (d, $^2J_{\text{PP}} = 20$ Hz, $^1J_{\text{WP}} = 221$ Hz, PMe₃). MS (EI) m/z : 1049 [M^+]. Anal. Calcd for $\text{C}_{35}\text{H}_{45}\text{O}_4\text{ClP}_2\text{W}_2\text{Si}_2$: C, 40.0; H, 4.32. Found: C, 40.59; H, 4.73. **4'b-SiW**: IR (ν_{CO} , THF): 2012 (m), 1908 (S), 1890 (S), 1876 (S) cm^{-1} . ^1H NMR (CDCl_3): δ 7.83–7.70 (m, 4H, C_6H_5), 7.60–7.38 (m, 6H, C_6H_5), 5.21 (m, 1H), 5.01 (m, 1H), 4.61 (m, 1H), 4.53 (m, 1H), 4.20 (m, 1H), 3.84 (m, 2H), C_5H_4 or C_5H_3 , 1.19 (d, $^2J_{\text{PH}} = 6.6$ Hz, 9H, PMe), 0.30 (s, 9H, Me), 0.14 (s, 9H, Me), -10.60 (s, $^1J_{\text{WH}} = 56$ Hz, 1H, W-H). $^{31}\text{P}\{^1\text{H}\}$ NMR (CDCl_3): δ 13.50 (d, $^2J_{\text{PP}} = 20$ Hz, $^1J_{\text{WP}} = 241$ Hz, PPh₂), -41.35 (d, $^2J_{\text{PP}} = 20$ Hz, $^1J_{\text{WP}} = 216$ Hz, PMe₃). Anal. Calcd for $\text{C}_{35}\text{H}_{45}\text{O}_4\text{ClP}_2\text{W}_2\text{Si}_2$: C, 40.0; H, 4.32. Found: C, 39.82; H, 4.83. **L = PPh₃ (5b-SiW)**: IR (ν_{CO} , THF): 2016 (m), 1915 (S), 1891 (S) cm^{-1} . ^1H NMR (CDCl_3): δ 7.72–7.45 (m, 25H, C_6H_5), 4.91 (m, 1H), 4.88 (m, 1H), 4.71 (m, 1H), 4.46 (m, 1H), 4.34 (m, 1H), 3.93 (m, 1H), 3.45 (m, 1H), C_5H_4 or C_5H_3 , 0.17 (s, 9H, Me), 0.10 (s, 9H, Me), -10.68 (s, $^1J_{\text{WH}} = 62$ Hz, 1H, W-H). $^{31}\text{P}\{^1\text{H}\}$ NMR (CDCl_3): δ 20.50 (d, $^2J_{\text{PP}} = 20$ Hz, $^1J_{\text{WP}} = 230$ Hz, PPh₂), 12.90 (d, $^2J_{\text{PP}} = 20$ Hz, $^1J_{\text{WP}} = 230$ Hz, PPh₃). Anal. Calcd for $\text{C}_{50}\text{H}_{51}\text{O}_4\text{ClP}_2\text{W}_2\text{Si}_2$: C, 48.54; H, 4.15. Found: C, 49.0; H, 4.96. **5'b-SiW**: IR (ν_{CO} , THF): 2016 (m), 1915 (S), 1891 (S) cm^{-1} . ^1H NMR (CDCl_3): δ 7.72–7.45 (m, 25H, C_6H_5), 5.06 (m, 1H), 4.95 (m, 1H), 4.65 (m, 1H), 4.56 (m, 1H), 3.92 (m, 1H), 3.64 (m, 1H), 3.44 (m, 1H), C_5H_4 or C_5H_3 , 0.26 (s, 9H, Me), 0.12 (s, 9H, Me), -10.61 (s, $^1J_{\text{WH}}$ masked, 1H, W-H). $^{31}\text{P}\{^1\text{H}\}$ NMR (CDCl_3): δ 20.72 (d, $^2J_{\text{PP}} = 20$ Hz, $^1J_{\text{WP}}$ masked, PPh₂), 12.60 (d, $^2J_{\text{PP}} = 20$ Hz, $^1J_{\text{WP}}$ masked, PPh₃).

Supporting Information Available: For **2b-CW**, **2b-SiW**, **3b-SiW**, and **3'b-SiW** tables of X-ray crystallographic data (including atomic coordinates, anisotropic thermal parameters, interatomic distances and angles, and least-squares planes) are available free of charge via the Internet at <http://pubs.acs.org>.

OM010495G